



Publication Year	2006
Acceptance in OA @INAF	2023-02-14T16:51:13Z
Title	NONLINEARITY INVESTIGATION AT 44 GHz USING PROTOTYPE UNITS: BEM44_B3_DC AND BEM44_B4_DC
Authors	CUTTAIA, FRANCESCO
Handle	http://hdl.handle.net/20.500.12386/33460
Number	PL-LFI-PST-RP-073



TITLE:

NONLINEARITY INVESTIGATION AT 44
GHz USING PROTOTYPE UNITS:
BEM44_B3_DC AND BEM44_B4_DC

DOC. TYPE:

TECHNICAL NOTE

PROJECT REF.:

PL-LFI-PST-TN-073

PAGE: I of V, 40

ISSUE/REV.:

DRAFT

DATE: March, 2006


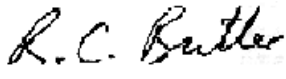

Prepared by	F. CUTTAIA LFI Project System Team	Date: March, 10 th , 2006 Signature: 
Checked by	LFI Project System Team	Date: Signature:
Agreed by	C. BUTLER LFI Program Manager	Date: Signature: 
Approved by	N. MANDOLESI LFI Principal Investigator	Date: Signature: 



TABLE OF CONTENTS

1	INTRODUCTION	6
2	DOCUMENT OVERVIEW	6
3	SCIENTIFIC PROBLEM AND SCOPE	7
4	TEST FLOW	8
5	BUILDING BEM CURVES	9
5.1	ATTENUATION CURVES USING POWER METER.....	10
5.2	ATTENUATION CURVES USING NOISE METER	12
5.3	EFFECTIVE ATTENUATION	12
6	COMPRESSION CURVES	14
7	1-DB COMPRESSION POINT	18
7.1	HOW TO READ THE COMPRESSION GRAPHS:	18
8	NOISE TEMPERATURE	20
8.1	NOISE TEMPERATURE CURVES	20
8.2	EXTRAPOLATION TO NON COMPRESSED CONDITIONS.....	21
8.2.1	<i>Results</i>	23
8.2.2	<i>Comparison with expected results</i>	23
9	FREQUENCY FILTERED CURVES	24
10	BEM RF USED AS NOISE SOURCE	27
11	FROM JBO TESTS TO RCA TESTS AND FLIGHT OPERATIONS	29
11.1	EXTRAPOLATION TO RCA CONDITIONS	29
11.2	4F2+ B3 ANALYSIS: JBO TEST VS. RCA_24 FM.....	33
11.3	EXTRAPOLATION TO FLIGHT CONDITIONS	35
11.4	T _{SKY} = 3K ± 100 MK.....	35
11.5	T _{SKY} = 3K ± 3 MK.....	37
12	SUMMARY	38
13	CONCLUSIONS	39



1 Introduction

Several tests have been performed at JBO to investigate the problem of representative FM BEM compression. Evidence of some compression happening inside the BEM is given by the high noise temperatures measured during the December test campaign, firstly on FEM 4F2 and then on FEM 4F3 when coupled to representative BEMs. JBO has four representative BEMs, two (B3 and B4) provided with diodes and then having a DC output, two (B1 and B2) without any diode and having an RF output. During last 2005 JBO tests, DC BEMs have shown to be compressed while RF BEMs have shown only a weak compression. Dedicated tests have been performed during the last test campaign to investigate the degree of compression, common features between the two BEMs, the noise temperature reachable in compressed conditions. Comparison tests have been also performed to check the repeatability of procedures used.

2 DOCUMENT OVERVIEW

§3 describes the scientific problem aiming this paper; §4 contains a flux diagram showing the test flow.

Output curves from the BEM are built using a variable power input: the different approaches followed to evaluate the effective power entering the BEM are reported in §5. Results are used as input to draw compression curves in §6: here a method based on 1st derivative analysis is proposed to investigate the local features.

1-dB compression point is investigated in §7: however, results show clearly that, cause the compression curve shape and the degrading experimental accuracy for high attenuations, it is impossible to define it unambiguously.

Noise Temperature is evaluated in §8 from independent data sets: cause the compression, the Y-factor method is unable to provide accurate results; noise temperature values are always much higher than what expected in conditions of linear response. Compression curves drawn in the previous paragraph are used here to correct high temperature voltages in order to apply Y-factor method directly to uncompressed data.

Compression could be generated from power coming from outside the nominal bandwidth: a waveguide filter is used in §9 to understand if compression can be ascribed to a bad filtering in the first LNA (IC1) or in the pass band filter mounted on the BEM.

§10 describes an attempt to build a 'synthetic' broad band source, representative of the FEM, using the prototype BEM44_B1_RF. Despite the same integrated power provided from the BEM44_B1_RF, results differ largely respect to those obtained using the FEM as powering source.

The last section of this document (11) is devoted to extrapolate results found with prototype BEMs to the FM RCA_24 detector. Two cases are examined separately: the behaviour during ground RCA calibrations and that during flight operations. In the first part (§11.1) compression curves are extrapolated to the operative range of RCA tests and are calculated also for the same configuration of RCA_24, that is using the FEM 4F2 instead of 4F3. In the second part (§ 11.3) results are instead extrapolated to in flight calibration range, when Jupiter or Dipole cross the detector's beam causing a fluctuation in the observed sky temperature. Scope of this section is that of evaluating the impact of non linearity in terms of gain and observed temperature variation.



3 SCIENTIFIC PROBLEM AND SCOPE

LFI radiometers are designed to work as square law detectors: it means that output voltage from the diode should be linearly proportional to the observed load temperature. JBO tests on representative FM BEMs demonstrated that the relation linking Voltage to Temperature is not linear. This feature impacts on Noise temperature and Gain evaluation. Any deviation from linearity is

Several tests have been dedicated to investigate BEM compression and to try to disentangle where compression is created. Actually, cause the BEM design, compression can happen in amplifiers 2, in the diode, in both of them.

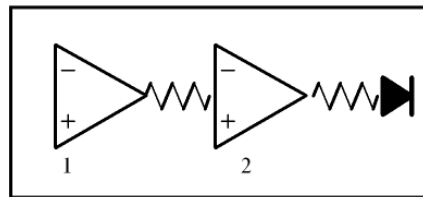


Figure 1 BEM electric schema

Square law diodes have a standard electric diagram as that shown in Figure 2: square law region is followed by linear law region, where voltage is proportional to square root of input power (load temperature).

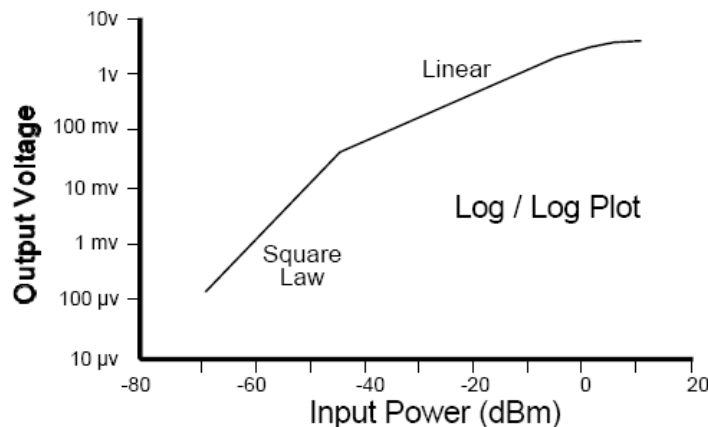


Figure 2 square law detector typical behaviour

The linear region is then followed by a region where voltage keeps near constant with increasing temperature.

Scope of this work is to clarify the operative region of the detector and try to quantify the compression; try to remove compression from data; extrapolate behaviour to RCA tests conditions and to flight conditions.



4 TEST FLOW

A schematic representation of the test flow is given in the diagram below. It contains three regions having a logical separation: on the left side, in light pink, are described the laboratory test performed; on the central region, in light blue, the analysis developed basing on data taken in the left side; on the right panel, in yellow, the scope of light blue analysis is described. Vertical and horizontal harrows indicate time and logical relation between two cells.

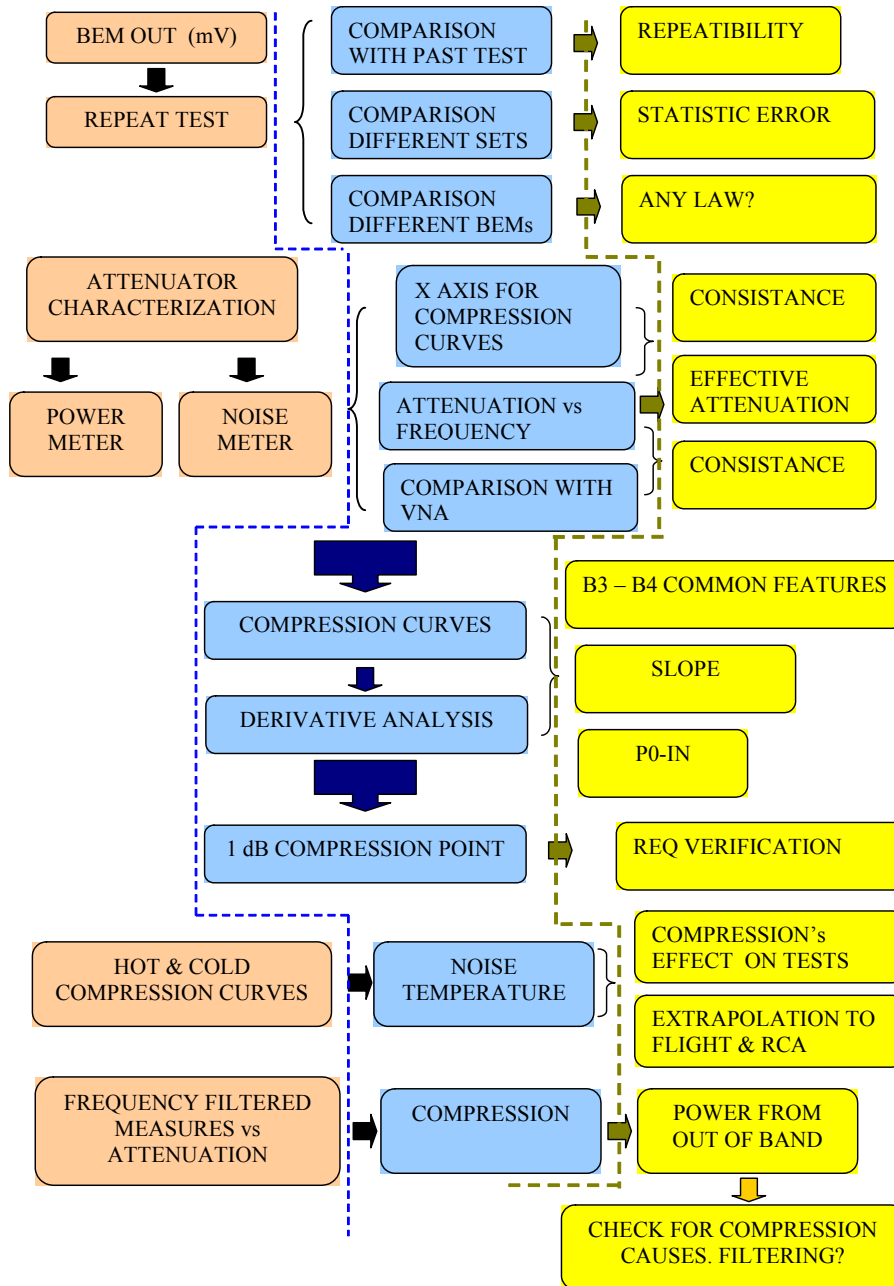


Figure 3 main test flow



5 BUILDING BEM CURVES

To investigate BEM output curves it is needed to feed the detector (BEM) using a variable power: this allows to relate the input power to the output voltage. A second step will be that of relating the input power to the load temperature.

BEM input was tuned using a variable attenuator, the same as used in December's test campaign and fully characterised in the next chapter, interposed between FEM and BEM that is coupled to a multimeter measuring output voltage. BEM output is here firstly represented versus the position read on the attenuator scale. It can allow to compare also with old data sets (December 2005) without making any guess on attenuation. For each curve, the absolute power level entering the BEM from the FEM (for that specific temperature and for that bias settings) is recorded using a power meter. Curves have been corrected for BEM offset.

BEM B3 Test Setup:
 $T_{SKY} = 25K$; $T_{REF} = 17.93K$; $T_{FEM}=20K$
BEM OFFSET 18.9 mV
BRANCH 1 LOSS: 0.85 dB
ABSOLUTE POWER INPUT: -48.8 dBm

BEM B4 Test Setup:
 $T_{SKY} = 25K$; $T_{REF} = 17.96K$; $T_{FEM}=20K$
BEM OFFSET 13.9 mV
BRANCH 1 LOSS: 0.85 dB
ABSOLUTE POWER INPUT: -48.8 dBm

Table 1 experimental setup

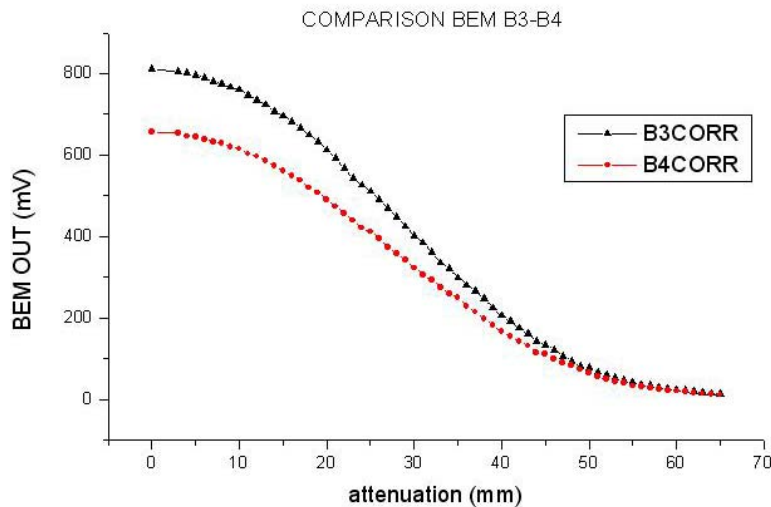


Figure 4 comparison between B3 and B4 response

The two BEM have a different constant mV/mW relating input power to BEM output signal: however, although the curve shape looks quite different; this representation could be misleading and normalized curves in §6 will be more exhaustive.

The B3 output curve can be compared with results of measurements taken during the December test campaign in JBO. Comparison shows a surprising excellent superposition of the two curves, indicating that the measurement has a good repeatability.

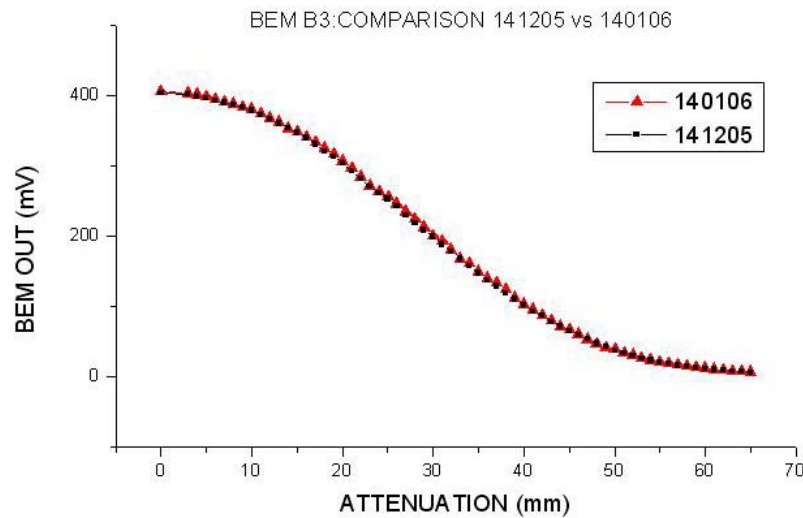


Figure 5 BEM B3: December 2005 vs. January 2006 curve

Attenuation curves have been measured in two ways:

- recording the integrated signal reaching the BEM flange, using a power meter;
- analysing the behaviour with frequency, using a noise figure meter.

5.1 attenuation curves using power meter

It is required to characterize the input power feeding the BEM. The approach followed during the Dicember test campaign foresaw the characterization of the variable attenuator using a Vector Network Analyser. Here a different way was followed to evaluate the net power entering the BEM using a power meter.

The attenuator is connected on a side to the FEM (4F3) hot waveguide exiting the cryo and on the other side to the power meter's diode. Power meter was previously calibrated using its internal reference source. It has a dynamic range up to -70 dBm, allowing to measure signals from the FEM attenuated until to -21 dB. Actually, the power exiting the FEM's flange is about -48.8 dBm (± 0.1 dBm).

Three independent measurements have been taken in different days and configurations, in order to have some statistic informations about repeatability. Different sets are compared in Figure 6: curves are in good agreement until position 53 (attenuation about -13.5 dB), then start to divert. This region, zoomed in Figure 7, represents the deviation from the average value as uncertainty bars.

More curves and relative tables are reported in ANNEX A

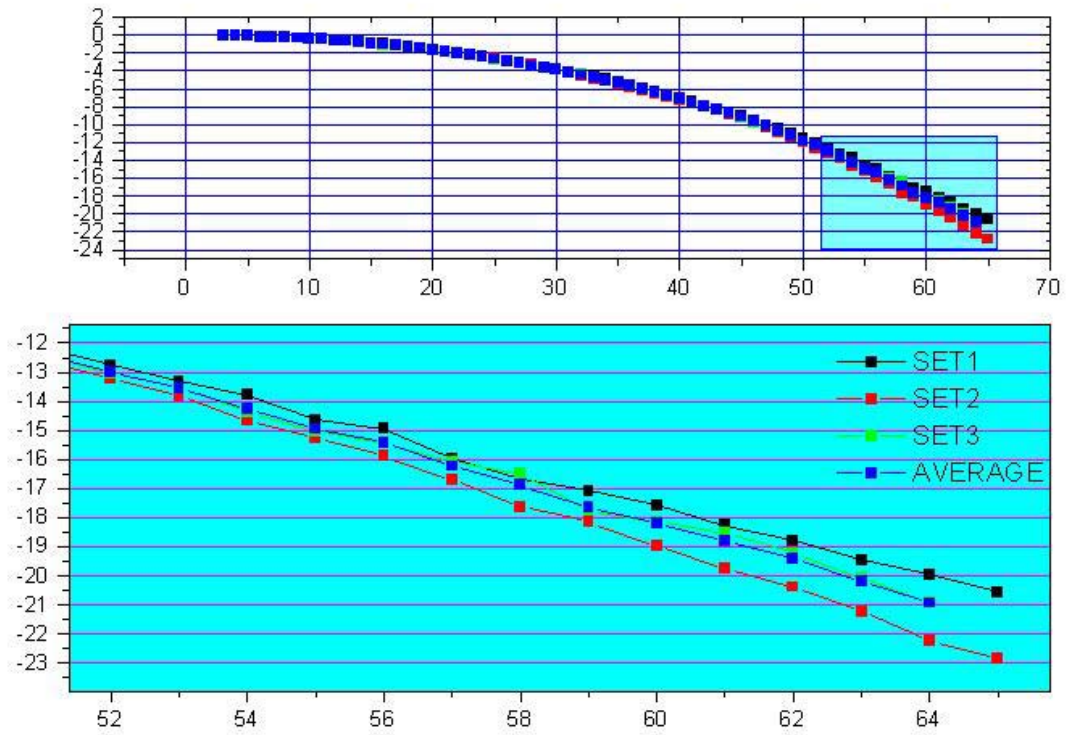


Figure 6 Zoom on the region where curves start to divert significantly (attenuation >13 dB, corresponding to position >53)

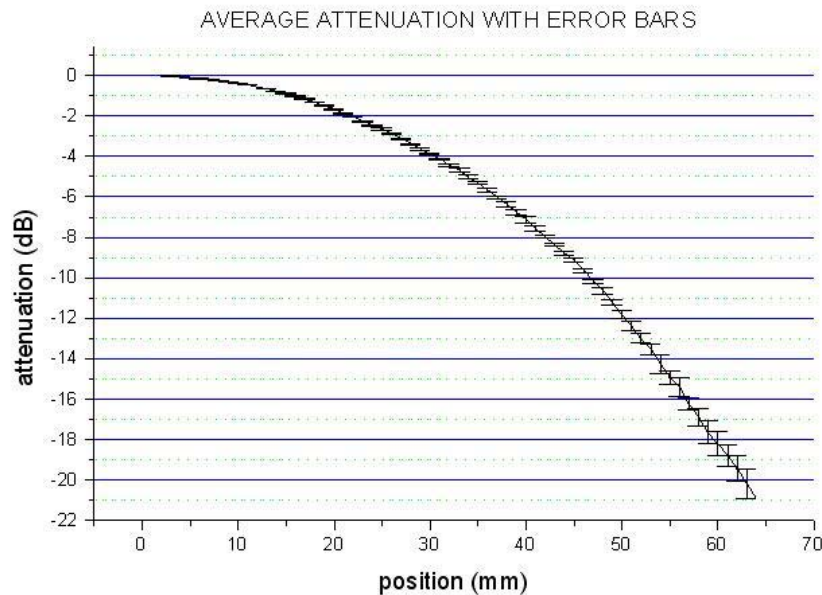


Figure 7 Curve attenuation vs. position: curve is obtained by averaging on the three sets of above. Error bars are displayed: they can be used as X-axis error bars in the compression curve plots of next chapters.



5.2 attenuation curves using noise meter

A Noise figure meter was used to measure power exiting the FEM for several positions of the variable attenuator, roughly corresponding to steps of 1 dB. Complete results are fully reported in ANNEX B. For each position values have been integrated along the bandwidth and compared with those obtained with power meter..

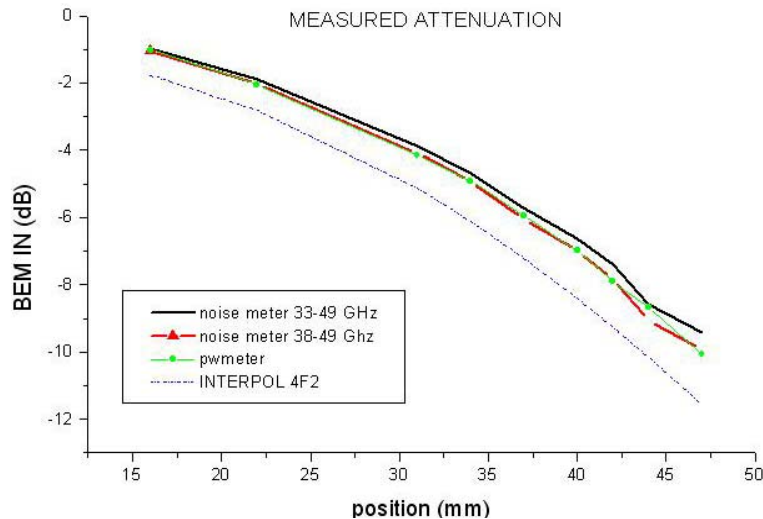


Figure 8 comparison between integrated power in two different intervals ([33 GHz – 49 GHz] and [38 GHz-49GHz]) using the noise meter and power detected using the power meter ([33 GHz – 50 GHz]; slight differences between noise meter and power meter can be ascribed to the non-identical interval spanned. The dot curve INTERPOL 4F2 corresponds to the November's analytic interpolation performed on 4F2 FEM when coupled to BEM B3. The absolute value of the curve is offset but the shape is similar. Offset is due to the different Gain of FEM used. Curve is reported only for completeness.

Values found with power meter are in very good agreement with those taken with noise meter (integrated along the band 38GHz- 49 GHz). (APPENDIX B). It enforces the choice to use these values. In ANNEX ** is also proposed the comparison with attenuation measured using VNA; curves show to have a good consistency.

5.3 Effective Attenuation

Theoretically, the effective attenuation (net power entering the BEM) should be calculated convolving in frequency the power exiting the FEM with the BEM insertion gain. Since the RF insertion gain is unknown (it was not measured in SAN), the effective attenuation of power entering the BEM, in first approximation, is assumed to be that measured with the power meter.

The uncertainty tied to this assumption can be quantified as the different attenuation if the full bandwidth (27 GHz- 50 GHz) or the nominal bandwidth (39.6-48.4 GHz) are considered.

Another indirect way is that of considering the insertion gain of the BEM RF B1, since it has been measured during this test campaign; however, also this approach is uncertain because of the different radiometric response of the RF and the DC BEM (as SAN people many times remarked). Despite all, results obtained by convolving the FEM out with the RF BEM insertion gain are very close to those from simply using the power meter over the full bandwidth.



To have an estimation of the uncertainty, attenuation will be evaluated in all the three cases. Complete values, together with insertion gain profile, are reported in tables # of APPENDIX B. A summarizing comparison is shown in Figure 9.

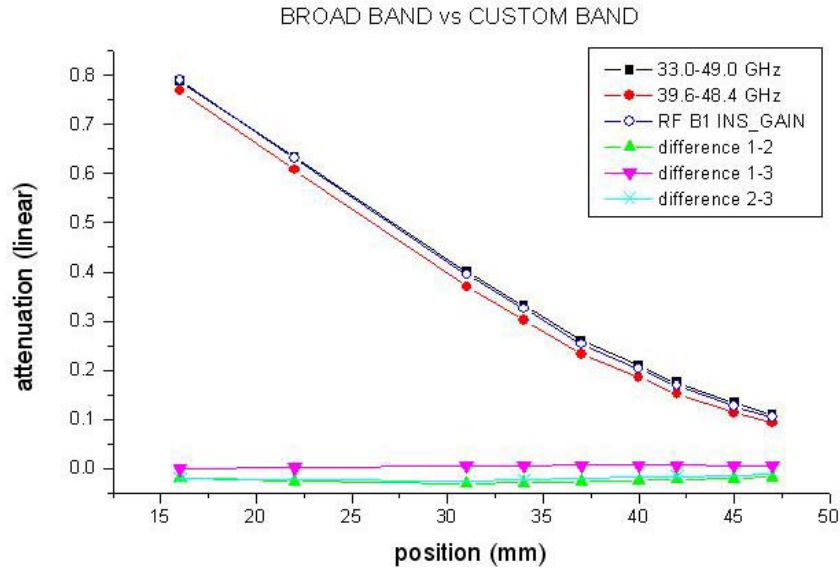


Figure 9 Comparison between full band measure (power meter, black solid square) nominal band measure (integrated power from noise meter, red trace, solid circle) and B1 insertion gain filtered measure (blue trace, hollow circle)

Comparison between the three approaches shows very small differences; the largest is between noise meter nominal band and power meter full band measure (named respectively 1 and 2) The absolute error committed considering one instead of the other is anyway smaller than 3%. Noise figure meter and power meter give comparable results, as shown by plot in Figure 10.

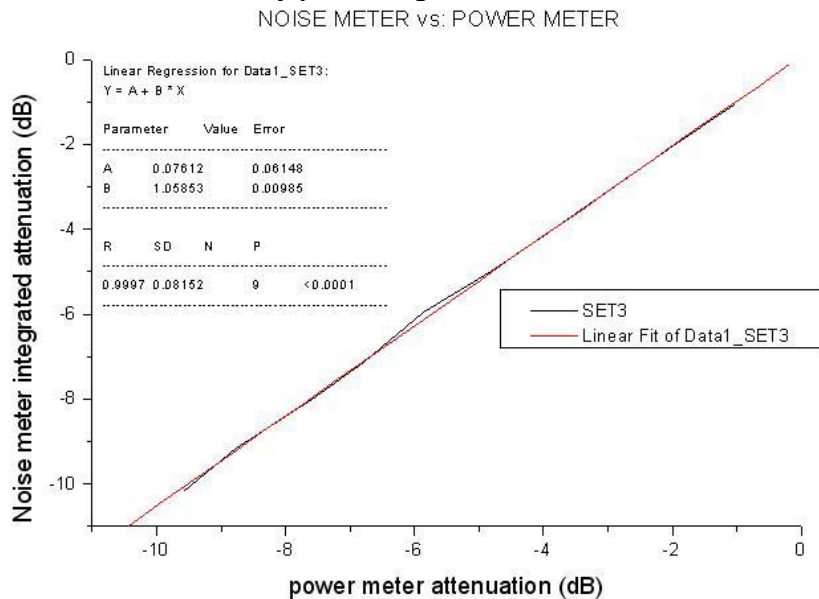


Figure 10 noise meter vs. power meter output: the good linear fit is the evidence of consistency between the two approaches.



6 COMPRESSION CURVES

In force of what established in the previous paragraph, the power meter's output (averaged over the three sets) is then chosen to represent the x-axis in the BEM compression plots.

Compression is calculated matching data from Figure 7 with B3 and B4 outputs given in Figure 4.

Power output is expressed in logarithm and normalized to the highest value, corresponding to 0-dB attenuation. In absence of compression, the log-log graph BEM out vs. attenuation should be a straight line $Y = A + B \cdot X$ with slope $B=1$.

In the next plots, the B3 and B4 compression curves are displayed together with a guess of linear fit: in both cases is $B < 1$. (B3: $B=0.88$; B4: $B=0.84$). Comparison between B3 and B4 normalized curves (Figure 11) shows quite common features.

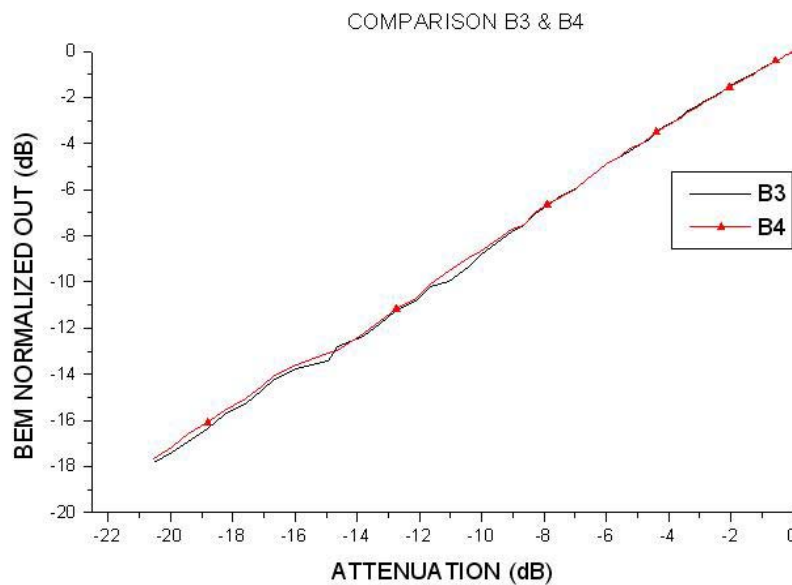


Figure 11 comparison between B3 and B4 compression curves.

A linear fit over the full range can not be representative of local linearity. Then, an analysis basing on the 1st derivative is proposed (Figure 14) to investigate if there are, also small, intervals showing a local common behaviour. This analysis can be used as starting point for the 1-dB compression point research.

B3 and B4 output are compared in Figure 12 by normalizing V to the 0-dB attenuation value (V_{MAX}) and differentiating with respect to normalized power in . Plot of V/V_{MAX} vs. normalized BEM input power P/P_{MAX} and of 1st order derivative follow for each BEM. The straight line is represented only to underline deviation from linearity.

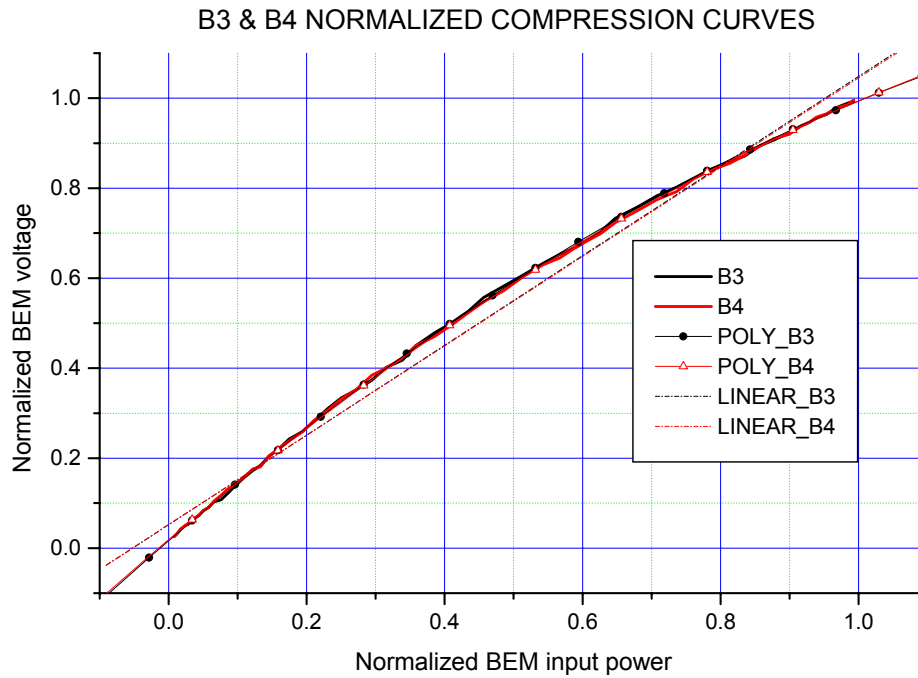


Figure 12 BEM B3 and B4 normalized linear compression. On X-axis the normalized BEM input P/P_{MAX} , on Y-axis the normalized BEM V/V_{MAX} output.

CURVE	BEHAVIOUR	EQUATION	A	Er (A)	B1	Er (B1)	B2	Er (B2)	R
BEM3	PARABOLIC	$Y = A + B1*X + B2*X^2$	0.0088	9.9E-4	1.234	0.0058	-0.346	0.006	0.99988
BEM4	PARABOLIC	$Y = A + B1*X + B2*X^2$	0.0191	9.6E-4	1.301	0.0057	-0.326	0.006	0.99988

Table 2

The derivative analysis is a powerful method to represent the regime in which the diode is working. The 1st derivative represents the local GAIN: a constant derivative means that the radiometer operates in the square law region ($V \sim A*T$); a regression $A * X^{-1/2}$ means that it works in the linear region $V \sim A*T^{1/2}$. A mixed regime can be represented by a parabolic behaviour, which derivative is a straight line. Different representative behaviours are reported in the figure below.

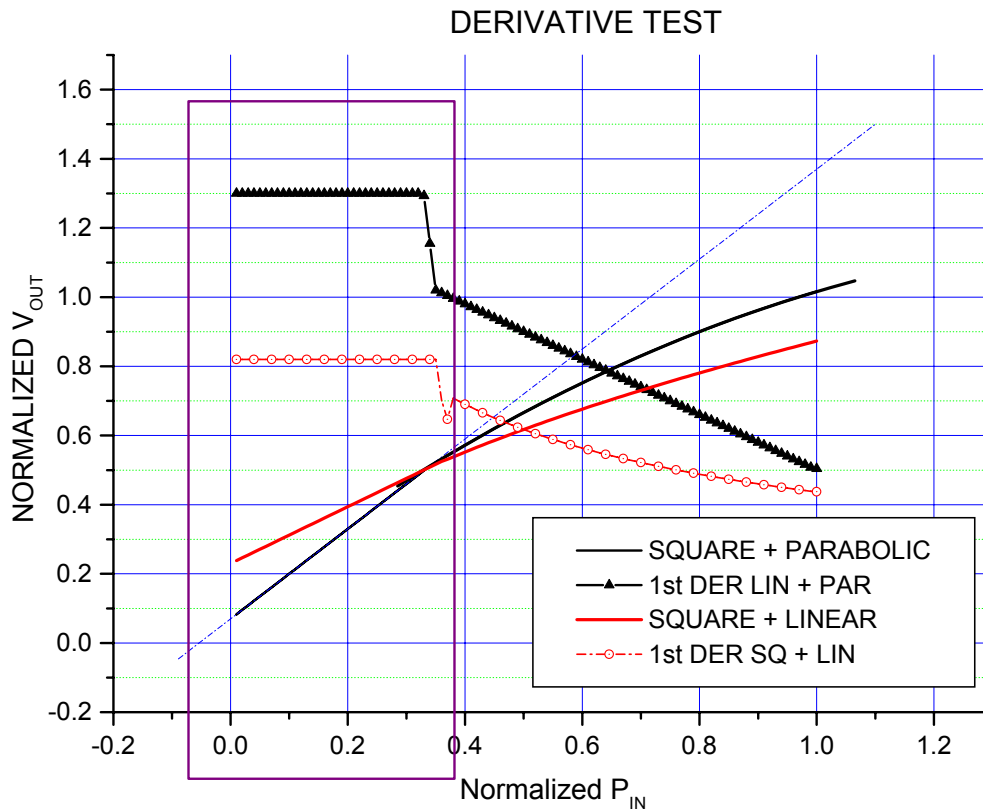


Figure 13 Simulated data: on x-axis is the normalized power entering the BEM, on y-axis the normalized voltage exiting the BEM; the red curve represents the normal behaviour for a square law detector: linear proportionality $V(P) = A \cdot P$ is followed by square root proportionality $V(P) = A \cdot P^{1/2}$. The black curves represent a detector working firstly in square law regime (linear proportionality) and then in a mixed compressed regime (parabolic regression)

The same procedure has been applied to real data, normalizing as above. However, we get only a monotone regression, without ever finding a region where the derivative is constant. This should indicate that the radiometer never works in square law conditions. Plots in Figure 14 have been obtained as derivative of plots in Figure 12.

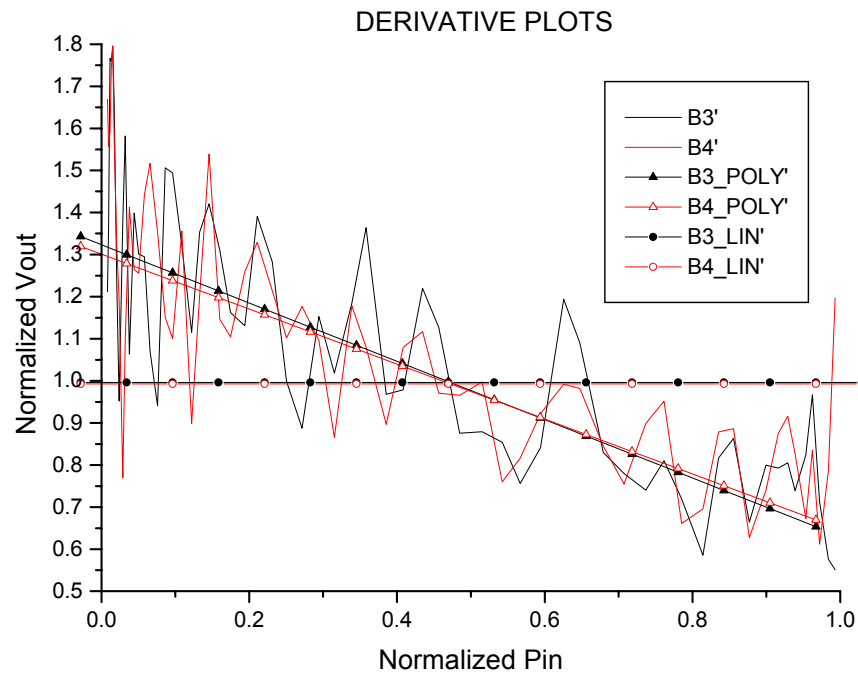


Figure 14 compression curves: derivative comparison. The curve $f' = \text{const}$ is completely inadequate to represent experimental data.

Also dividing each curve in several regions to make separate fits, we can not find any region where the first derivative is a constant. At the first look, a guess could be made (as it happens in the example of Figure 13) trying to fit the first region $x = [0 - 0.2]$ with a straight line $y = \text{const} \sim 1.25$ and the second region $[0.2 - 1]$ with a linear regression; in this case, it should mean that the diode works in a quadratic-like regime until ~ -7 dB (corresponding to ~ -55.8 dBm) and then starts to work in compressed linear regime. However, given the very irregular shape of the curve, this interpretation seems to be largely hazarded and any attempt to reproduce this behaviour fails.

Actually, the curve best fit seems to be, also locally, a linear regression with slope $m = -0.69$. if this is true, it would mean that the BEM never works in quadratic regime but in a mixed state of quadratic and linear region. Actually, neither the $V(P) = G \cdot P^{1/2}$ and the $V(P) = G \cdot P$ plots are able to represent the detector features: its behaviour, besides that by a parabolic fit, can be approximated by a power law $(V) = G \cdot P^{1/a}$ with $1 < a < 2$.



7 1-dB COMPRESSION POINT

The 1-dB compression point should operatively be calculated recording voltage moving from the square law region (linear dependence V-P) of the detector and increasing power until the compression starts, that is where the curve changes slope (in the derivative plot). From now this point will be named P0-in reference point .

We are not able to identify in derivative graphs a constant region $y = \text{const}$ corresponding to a linear region in BEM out plot.

An attempt to define compression is done considering the full attenuation curve (logarithmic). On X-axis is the BEM input power attenuation (normalized to the 0-attenuation power), on Y-axis the BEM compression. it is measured as:

$$\mathfrak{S}(i) = (P_i - P_0)dB - (V_i - V_0)dB$$

As is in Figure 12, BEM B3 and B4 show general common features.

7.1 How to read the compression graphs:

Compression curves are represented in Figure 15: they can be read as it follows. Each plot displays three curves, labelled as 'MIN', 'AVE', 'MAX'; they represent the three different characterizations of the attenuator given in §5.1 (SET1, SET2 and AVERAGE, Figure 6 and Figure 7)'.

On X-axis is the normalized attenuation (0 dB corresponds to $T_{sky} = 25$ K); on Y-axis is the total compression $\mathfrak{S}(i)$.

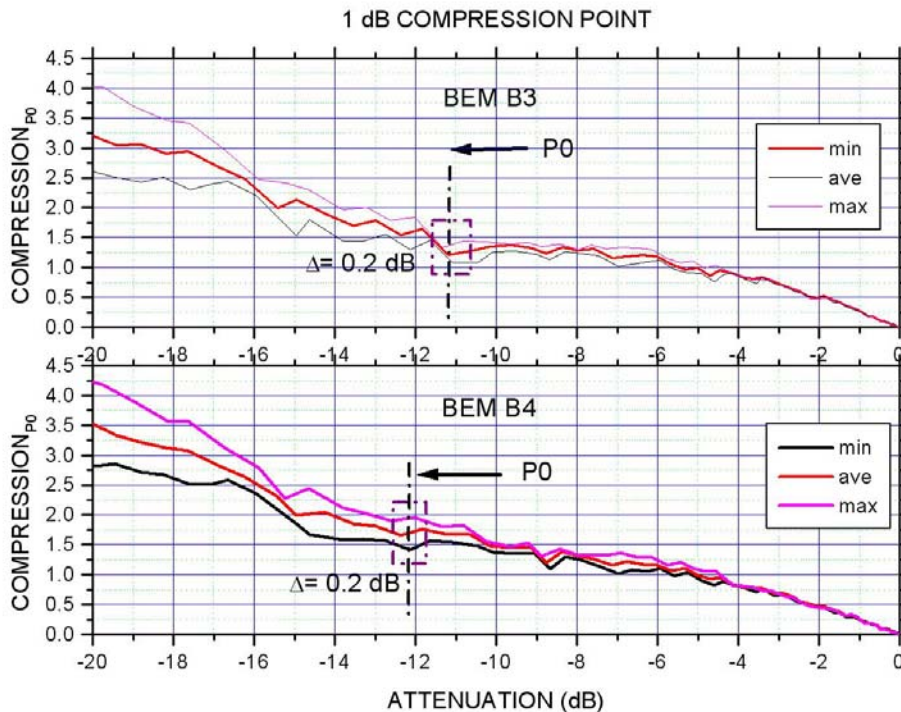


Figure 15



Since the initial choice of P_{0-in} affects strongly the final result, it is proposed here a dynamic method to evaluate the compression point. It is also worth of noting that the higher the attenuation the larger is the uncertainty due to attenuation estimation ; moreover, it must be added that a for radiometer having typical Noise Temperature of ~ 15 K looking a load hold at 25 K, the input range [25 K-0 K] is [0 dB : -4.26 dB]: so, it is useful to attenuate until -20 dB only as a test of BEM compression but it does not represent any real case (since both the load and the radiometer noise temperature are lowered by a factor 100).

Since the power meter accuracy degrades for $P_{in} < -12$ dB, we can try to investigate the behaviour in the range [0 dB: -11 dB] to search for a flat compression region. This region corresponds to power input: [-49 dBm : -60 dBm].

Figure 16 shows that, if this region exists, it is actually very narrow and can not be considered as representative of a linearity region.

However, if, as exercise, we assume that in the region $P_{in} < -12$ dB the BEMs are working close to square law regime, we get:

compression	B3	B4
Total (25K) dB	1.39	1.71
1-dB (power in)	-1.03 (-49.43 dBm)	-3.08 (-51.43 dBm)

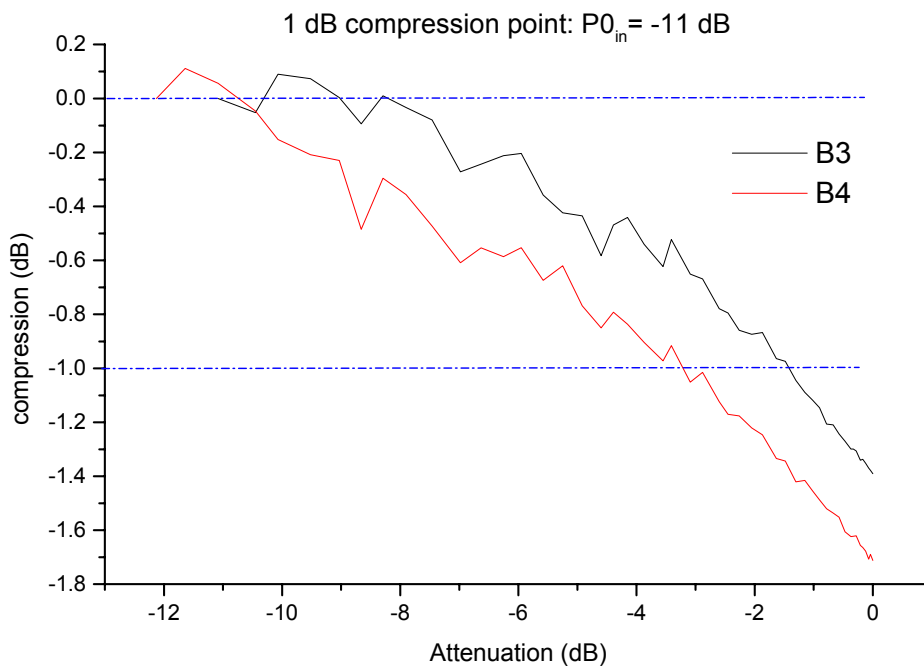


Figure 16

It is clear from the above graph that, also if it is assumed that the BEMS are not compressed for $P_{in} > -60$ dBm, however a slight, but almost constant, compression is shown.

Results show that it is very difficult in this conditions to define the 1-dB compression point: it seems to be useful only from a formal point of view but it does not provide any more information useful to manage the compression problem; indeed it could provide misleading results depending on the choice done for P_{0-in} .



8 NOISE TEMPERATURE

8.1 Noise temperature curves

Compression affects strongly also the Noise Temperature evaluation, when the Y-factor method is used. BEM OUT (B3 and B4) have been independently registered for several values of P-in attenuation. Voltages have been recorded for $T_{SKY} = 25K$ and $T_{SKY} = 35K$.

For each BEM, two noise curves are plotted (see Figure 17), considering or not the non-isolation correction (due to reference load temperature changes).

The two BEM seem to have similar feature: the noise temperature curve has a U-shape, with a minimum several dB higher than the FEM stand-alone value. Both the curves have irregular shape, probably due to the uncertainty tied to the Y-factor method application: actually, also a small error committed in re-positioning the attenuator passing from Hot (35K) to Cold (25K) state can cause a large error in Y and then in T.

In Both cases, the minimum seems to be located in the region comprised between attenuation -6 dB (BEM 4) and -8 dB (BEM 3).

The U-shape is mainly due to two factors:

- Compression
- Attenuation

The over-all behaviour has been reproduced by simulating the system (purple curve with filled circles in Figure 17). The high uncertainty tied to input power estimation suggested to start the simulation at $X = -15$ dB.

Different compression levels in the hot and cold state are responsible of the low-attenuation region behaviour; The V-P (Volt – Watt) curve has been supposed to follow a law : $Y=C+A*X- B*X^2$; hot and cold state are then supposed to be differently compressed, by an amount proportional to $(T_{HOT}-T_{COLD})$.

Attenuation is responsible of the high-attenuation region behaviour in different ways:

- lowering the FEM gain G, the ratio BEM_noise/G increases.
- The attenuator, that here is a waveguide attenuator, emits by an amount proportional to its thermodynamic temperature (300K) and to its attenuation.

Looking the simulated uncompressed curve (black curve) it is possible to appreciate the separated effect of attenuation. Changing the relative coefficients and temperatures, you can change the level of the left or right side of the curve.

It arises from the plot below that:

In every case of compression the Y-factor method is not a suitable estimator for Noise Temperature. It provides results **as much far from the real value as the temperatures used (hot and cold state) are far:** actually, relative compression between two states changes by an amount proportional to their temperature difference.

Each BEM has its own compression curve; curves have all a similar shape but with different maxima and minima.

Minimum is located for all the curves approximately in the same position, that is predictable taking into account compression and attenuation.

Curves found using the Y-factor method are very irregular, due to the strong sensitivity of this method on uncertainty due to attenuator positioning.

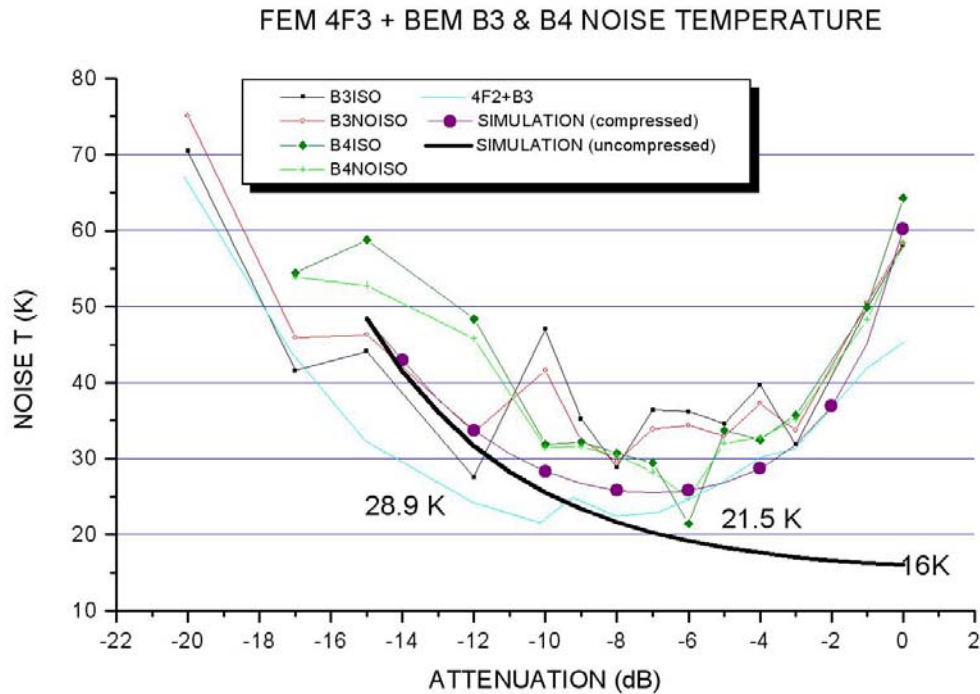


Figure 17

8.2 Extrapolation to non compressed conditions

Here it is described an attempt to correct Noise temperature data taking into account compression: correction will be applied directly on the high temperatures voltages, basing on compression curves for BEM B3 and B4 given in the previous chapters.

Curves are expressed in terms of linear normalized power input (X axis) vs BEM output in mV (Y axis), following the same representation given in Figure 12.

Experimental curves are both fit with 2nd order polynomial regressions:

$$Y = C_{\#} + B_{\#}X - A_{\#}X^2$$

Where # is the BEM number.

The x axis is expressed linearly as a fraction of power input at 25 K.

It is here to be remarked that when you apply an attenuation after the FEM you are simultaneously attenuating both the load temperature and the FEM Noise temperature. It will be taken into account in the correction.

The two fits used are:

$$B3 \quad V \text{ (mV)} = 7.15 + 1081.81 * P - 283.07 * P^2$$

$$B4 \quad V \text{ (mV)} = 8.33 + 859.44 * P - 215.62 * P^2$$



The BEM offset contributions have been already removed from these curves.

All coefficients must be normalized to $V(25\text{ K})$, since each state of the phase switches has a different V_{OUT} but the shape of the curve is the same. V_{OUT} can moreover depend on the BEM temperature and on other factors.

We are interested to the quadratic correction coefficient \tilde{A} , then :

$$\tilde{A}_3 = A_3 / [V(25\text{K})_{B3} - \text{offset}(B3)]$$
$$\tilde{A}_4 = A_4 / [V(25\text{K})_{B4} - \text{offset}(B4)]$$

Noise Temperature has been evaluated between 25 K and 39.9 K:

The linear increasing in Power input with respect to 25 K is:

$$\Delta_{\text{Pin}} = \text{Pin}(25\text{ K}) / \text{Pin}(39.9\text{ K})$$

Where:

$$\text{Pin}(25.0\text{ K}) = \text{TN}_{\text{FEM}} + \text{TLOSS}_{\text{WG}} / \text{G}_{\text{FEM}} + 25.0$$
$$\text{Pin}(39.9\text{ K}) = \text{TN}_{\text{FEM}} + \text{TLOSS}_{\text{WG}} / \text{G}_{\text{FEM}} + 39.9$$

All the quantities below are evaluated for a given phase switch state:

$$\text{TN}_{\text{FEM}} = \text{Noise Temperature evaluated for the FEM alone}$$
$$\text{TLOSS}_{\text{WG}} = \text{physical temperature of waveguides multiplied times their average loss}$$
$$\text{G}_{\text{FEM}} = \text{FEM average gain}$$

Then, if $V_{@}(25\text{K})_{\#}$ and $V_{@}(39.9)_{\#}$ are respectively the compressed voltages measured at 25 K and 39.9 K for the BEM $\#$, the corrected value can be obtained adding the quadratic term that avoided the fit to be linear:

$$\tilde{V}_{\#} = V_{@}(39.9\text{ K})_{\#} + \tilde{A}_{\#} * [V_{@}(25\text{ K})_{\#} - \text{offset}(B_{@}\#)] * (\Delta_{\text{Pin}})^2$$

Where: $B_{@}\#$ is the BEM $\#$ offset evaluated in correspondence of $V_{@}$

For 4F3 tests is:

$$\text{offset}(B3) = 18.9.3\text{ mV}$$
$$\text{offset}(B4) = 13.9\text{ mV}$$
$$V(25\text{K})_{B3} = 810.9\text{ mV}$$
$$V(25\text{K})_{B4} = 656\text{ mV}$$
$$A_3 = 283.1$$
$$A_4 = 215.6$$

TN_FEM:

$$\text{LNA1\&4} = 15.5\text{K for both AB/BA}$$
$$\text{LNA2\&3} = 17.5\text{K for both AA/BB}$$

$$\text{TLOSS}_{\text{WG}} = 300\text{K} * (0.63) = 189.3\text{ K}$$
$$\text{G}_{\text{FEM}} = 31\text{ dB (for all PH}_{\text{SW}} \text{ states and OP)}$$



For G_FEM of the order of 30 dB the TLOSS_WG contribution becomes negligible.

Once Hot states voltage have been corrected, standard equations are used to evaluate isolation (ISO) and Noise temperature (Tn), as usual.

ISO is taken without any correction (compression should only marginally affect this term); Tn is calculated considering ISO correction as follows:

$T_n^* =$

$$\frac{[t_{c_1}^2 - t_{c_1} * t_{c_2} * (Y1 + Y2) + t_{c_2}^2 * Y2 * Y1 - t_{hot1}^2 + t_{hot2} * (t_{hot1} * (Y1 + Y2) - t_{hot2} * t_{c_2} * Y1)]}{[t_{c_1} * (Y1 + Y2 - 2) + t_{c_2} * (Y2 - Y1 * (2 * Y2 - 1)) - t_{hot1} * (Y1 + Y2 - 2) + t_{hot2} * (Y1 * (2 * Y2 - 1) - Y1)]}$$

Tc_1 is the reference load temperature when SKY is in the state HOT

Tc_2 is the reference load temperature when SKY is in the state COLD

Y2 and Y1 is the Y-factor evaluated for states AB and BA (LNA1&4) and AA and BB (LNA2&3)

Correction has been applied to last measurements performed at JBO on 4F3 (data_set_XXX, February 2006)

8.2.1 Results

Results are shown in the table below:

CHANNEL	COMPRESSED	CORRECTED
1	62.0 K	17.1 K
2	56.9 K	16.2 K
3	73.0 K	18.7 K
4	66.0 K	18.5 K

Table 3 results from compression correction

8.2.2 Comparison with expected results

A first rough model has been implemented in order to take simultaneously into account both compression and attenuation due to losses in the transmission line connecting the FEM to the BEM. Details of this work will be added here or inside a separate document. It is to be noted here that corrected Noise Temperatures are in good agreement with model within 0.8 K.

TBC



9 FREQUENCY FILTERED CURVES

This section try to answer this question: **can compression be ascribed to a power excess due to a bad filtering in the BEM?** Can a power excess from the region out of the nominal bandwidth (< 39.6 GHz; >48.4 GHz) cause saturation in the IC2 LNA or in the diode?

A waveguide filter has been used to check it.

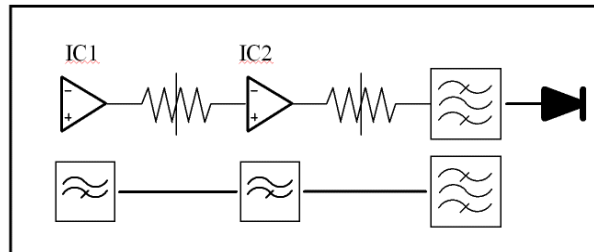


Figure 18 BEM electrical drawing: in the upper part are represented: the IC1 and IC2 HEMT low noise amplifiers, two attenuators, filter, diode. In the lower part the filtering characteristics are described: IC1 and IC2 behave as pass-high filters, the filter between attenuator 2 and diode is a pass-band filter.

The BEM behaves as a filter in two steps: LNAs IC1 and IC2 contained in the BEM behaves pass-high filters with a certain insertion gain . The second filtering happens between IC2 and the diode and is demanded to a pass band filter. However, RF characteristics of DC BEMs B3 and B4 are not well known: it means that the actual power entering the BEM is not easily and accurately computable. This lack avoids to estimate the effective power causing the compression: we know the power exiting the FEM in the region [33 GHz – 50 GHz] (about -48.8 dBm at the BEM flange) but we do not know its amount rejected by the first and second filtering.

A pass band filter, [39.6 Ghz-48.4 GHz] which profile is described in Figure 20, has been used to estimate:

- The net power entering the BEM from outside the filter pass-bandwidth .
- The actual compression level, supposing that the total power exiting the filter enters the BEM.
- If after waveguide filtering the compression disappears, it means that the compression can be ascribed to a bad filtering in IC1.

Besides of nominal characteristics provided by the manufacturer, given in Figure 20, the insertion gain of the filter has been measured in nominal working conditions, by difference, using a Noise Meter and the FEM as power source. The attenuation profile (Figure 20) is obtained by subtracting the power exiting the FEM coupled to the noise meter and that reaching the noise meter when the filter is interposed.

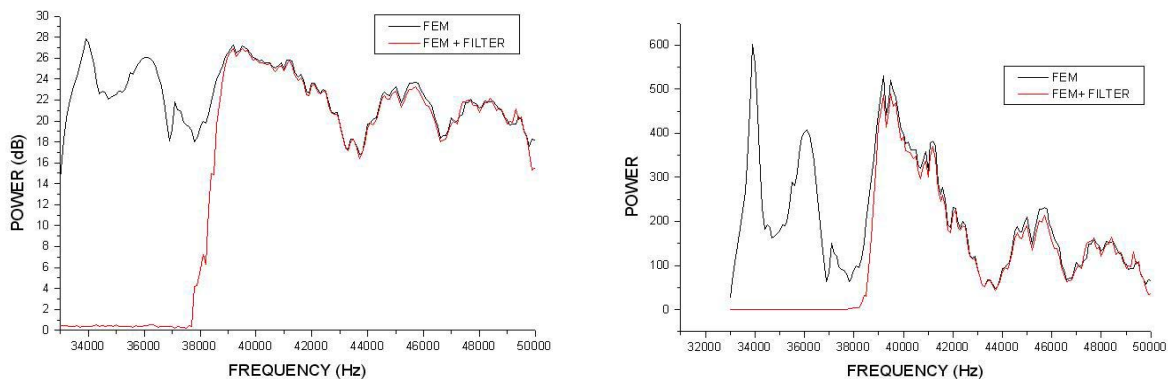


Figure 19 waveguide filter: logarithmic (left panel) and linear (right panel) insertion gain compared with FEM S₁₂

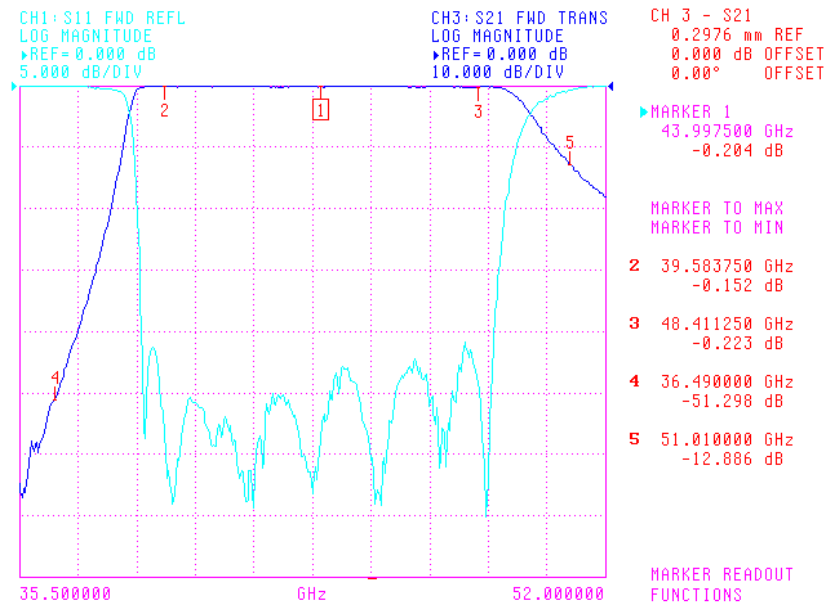


Figure 20 waveguide filter: S_{11} and S_{12} curves provided by the manufacturer

Evaluating the ratio

$$\mathcal{R} = P/P_{\text{FILT}}$$

between Integrated power exiting the FEM before and after filtering we know the power decreasing due to filtering. Test is performed in the bandwidth 33-50 GHz, so result represents the lowest case. It is expected that, if compression is due to a large power from outside the bandwidth, the ratio:

$$\mathcal{V} = V/V_{\text{FILT}}$$

be, in linear conditions, of the same order of \mathcal{R} or larger. Instead, if it is lower, it can mean either that:

- i) compression has not been removed by interposing the attenuator: the detector is still working in non-linearity conditions
- ii) power coming from outside the filter does not enter the BEM and does not contribute to its output.

Integration from Figure 20 provides the following results:

Integration of Data1_FEM:				
i = 1	-->	171		
x = 33000	-->	50000		
Area		Peak at	Width	Height
3.51681E6		33900	600	602.28
Integration of Data1_FEM+FILTER:				
i = 1	-->	171		
x = 33000	-->	50000		
Area		Peak at	Width	Height
2.15998E6		39500	2900	488.43

Table 4

RATIO FILTERED/NON-FILTERED: $\mathcal{R} = 0.614187$
 $\mathcal{R}_{\text{LOG}} = -2.117 \text{ dB}$



Ambiguity of point i) has been removed recording BEM output for several values of attenuation both for unfiltered and filtered setup: it allows to find, if it does exist, the attenuation required to get the right ratio \mathcal{R} .

The Plot below (Figure 21) shows that the BEM output is only weakly perturbed by interposing the filter: \mathcal{R} is in both cases higher than \mathcal{V} , also for large attenuations. It means that the power reaching the BEM B3 and B4 comes, from a region fully comprised in the bandwidth 33GHz-50GHz and also smaller. Moreover, B4 seems to have a pass-bandwidth narrower than B3. As already found previously, B4 shows a larger dependence on attenuation denoting a stronger compression.

	\mathcal{V} Mean	\mathcal{V} Mean (dB)	sd(YEr \pm)	se(YEr \pm)	N
B3	0.7641	-1.1685	0.02386	0.00638	14
B4	0.8455	-0.72886	0.03551	0.00949	14

Table 5

It must be considered, only for completeness, that, if the BEM filter would exactly the same pass-high profile of the waveguide filter, then respectively only 1.16 dB (BEM 3) and 0.72 dB (BEM 4) could come from the region >48.4 GHz. This numbers represent a worst case.

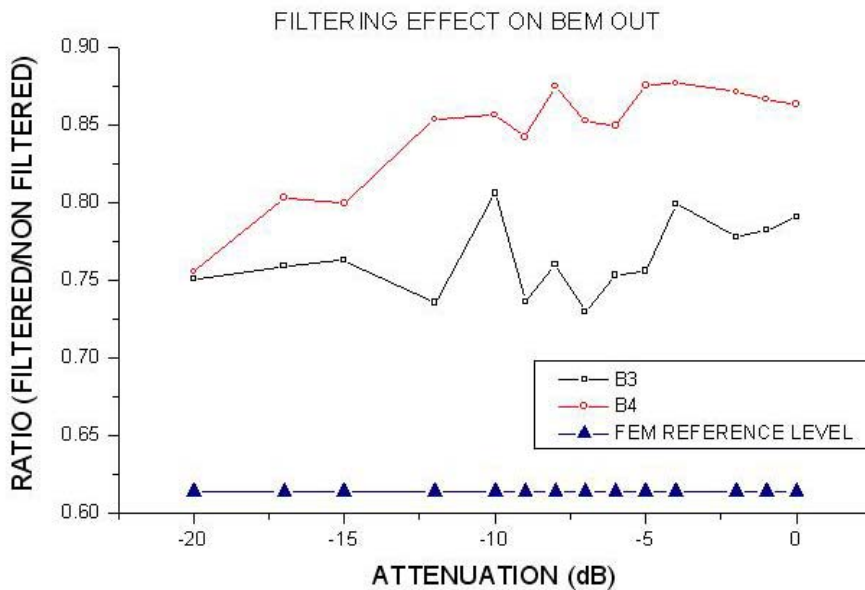


Figure 21



10 BEM RF USED AS NOISE SOURCE

An attempt to build a 'synthetic' broad band source has been done using the representative BEM RF B1. It was firstly characterised from a RF point of view and than employed joined with the variable attenuator and the DC BEM, following the schema reported in the picture below.

The scope is double:

- Looking for a broadband source representative of the FEM.
- Checking if the integrated total power entering the BEM has a one to one correspondence with the compression level.

The answer has been in both cases negative.

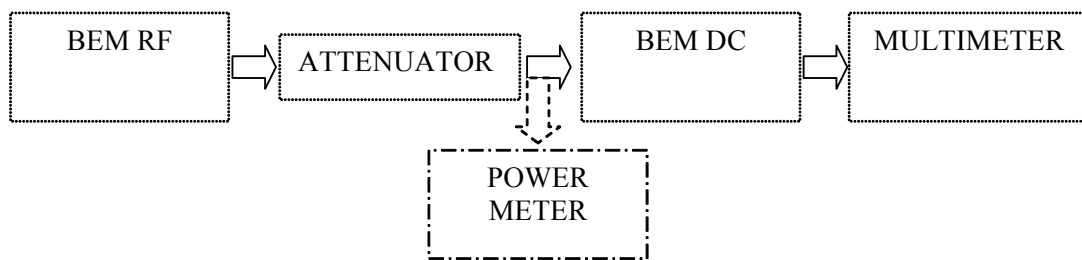


Figure 22

The power exiting the attenuator is monitored connecting a power meter instead of the BEM DC; an attempt to use a directional coupler to monitor in real time the power exiting the attenuator did not provide good results because of the 12 dB loss in the second branch of directional coupler that push performances very close to the dynamic limit of the instrument. (dynamic range -70 dBm; the power input must be -48.8 dBm; being the LOSS in the directional coupler -12 dB, it implies that it would be allowed to attenuate only by less than 9 dB).

Without any attenuation or filtering, the power exiting the BEM is -46.64 dBm. It is necessary to attenuate about 2 dB to get the power level exiting the FEM at 25 K (-48.8 dBm). It is obtained positioning the variable attenuator on 22.

However, the voltage at the terminals of the BEM is 1114 mV (balanced condition) while, if the same Pin= -48.8 dBm comes from the FEM, it gives 935.4 mV. To have the same output it was needed to attenuate until Pin= -50.65 dBm

	Pin (dBm)	OUT (mV)	Pin (dBm)	OUT (mV)
FEM 4F3	-48.8	935.4	-50.65	677.7
BEM B1	-48.8	1114	-50.65	935.4

Table 6

The same test is repeated also filtering the BEM RF B1 output using the same filter as in the previous paragraph.

	Pin (dBm)	OUT (mV)
BEM B1	-48.8	1075

Table 7

The output found is very close to that obtained without filtering (R is about 0.97, corresponding to a difference of about 0,2 dB in Pin)

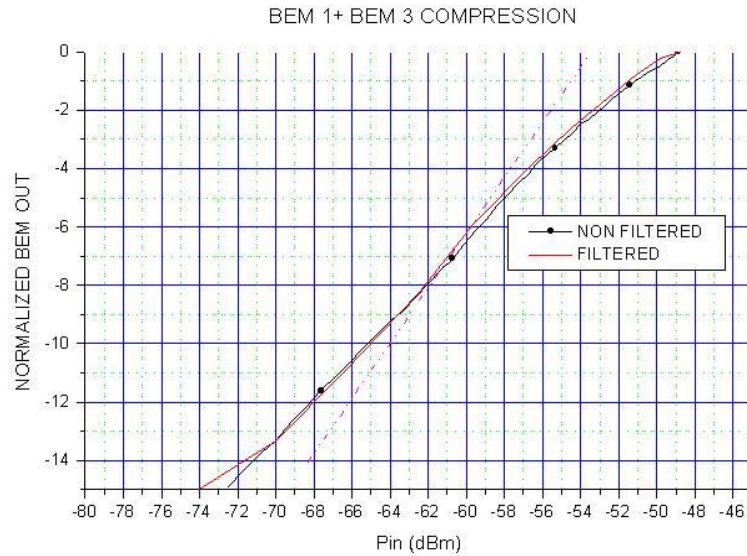


Figure 23

It is worth of noting that, after the renormalization (allowing to superpose the 0-attenuation point of the two curves), the Filtered and non-filtered compression curves are very similar. Also in this case it means that the BEM DC is filtering properly and that all the compression is due to power coming from the nominal bandwidth. The dot-dashed magenta straight line represents the theoretical non compressed behaviour, that is very far from the actual.

Only for comparison, if we consider chose $P_{0-in} = -10$ dB, we can also compare with FEM+BEM compression curve.

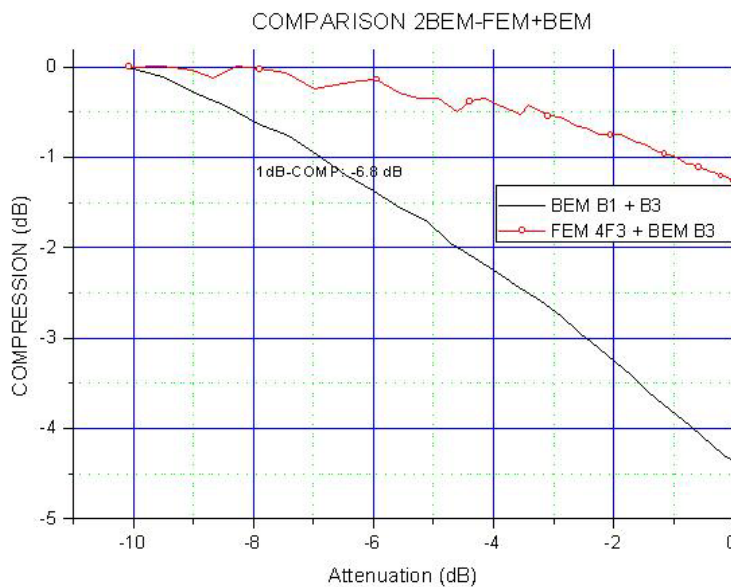


Figure 24

From the Plot it is clear that the BEM B3 compression depends strongly on the power source used. What matters is not only the P_{in} level but also the shape of the gain curve and then the S-parameters matching with the BEM.

This result suggests also that a **CW single tone analysis of the compression point, based only on the P_{in} level, can not be representative of the overall compression in broad-band regime.**



11 FROM JBO TESTS TO RCA TESTS AND FLIGHT OPERATIONS

Results obtained in the previous chapters can be managed to predict the BEM behaviour at level of RCA tests and of flight performances.

The three following paragraphs show that it is possible to extrapolate performances from compression curves obtained with prototype BEMs to instrument level tests and to flight conditions operation (mainly calibration operations)

11.1 Extrapolation to RCA conditions

Results from compression tests can be extrapolated to RCA tests transforming the input power into thermodynamic temperature of the observed load (T_{SKY}). In doing this, it must be taken into account that the power entering the BEM from the FEM is composed of two terms: the power from the LOAD and the power from the FEM noise temperature.

When attenuation is increased from 0 dB to -20 dB, also the Noise temperature is attenuated together with the sky component. So, if $T_{sky} = 25$ K and T_n is supposed to be about 15 K, attenuation of -20 dB does not produce any realistic situation, being:

$$-20 \text{ dB} = (T_{SKY} + T_n) / 100 \sim 0.04 \text{ K}$$

RCA test should span the range : $T_{SKY} = [3\text{K}-25\text{K}]$; however, due to the cryogenic setup limits, only the range $T_{SKY} = [8\text{K}-30\text{K}]$ have been investigated.

The first thing to do is that of select the operative range in power:

If the noise temperature of FEM in stand-alone tests is T_n , and if X is the linear power input, i.e:

$$X = 10^{(A/10)},$$

where A is the attenuation, then:



$$T(K) = (T_n + 25K) * [X - T_n / (T_n + 25K)]$$

It is clear that we are able to represent T axis as well as we know the FEM alone noise temperature. However, the final results, providing system noise temperature and Gain, are not strongly dependent on this parameter, at least within the uncertainty of a couple of Kelvins.

Normalized compression curves from Figure 12 have been here represented with respect to Sky temperature variation. Assuming $T_n = 15K$, the power range explored is [0 dB : -4.25 dB] corresponding to the thermal range: $T_{SKY} = [25K : 0K]$.

In uncompressed conditions the linear relation Voltage –Temperature provides symmetry in the V-T representation.

Indeed, if $V = a + G * T$, gain can be found as:

$$G = dT / dV$$

or alternatively as :

$$G = 1 / (dV/dT)$$

If the relation between V and T is nonlinear, the value found for G depends on the representation given, as the Noise Temperature.

The same approach of RCA tests is followed here, giving both the representations and averaging between results. Results are displayed in Figure 25. For simplicity the analysis is performed here only on BEM B3.

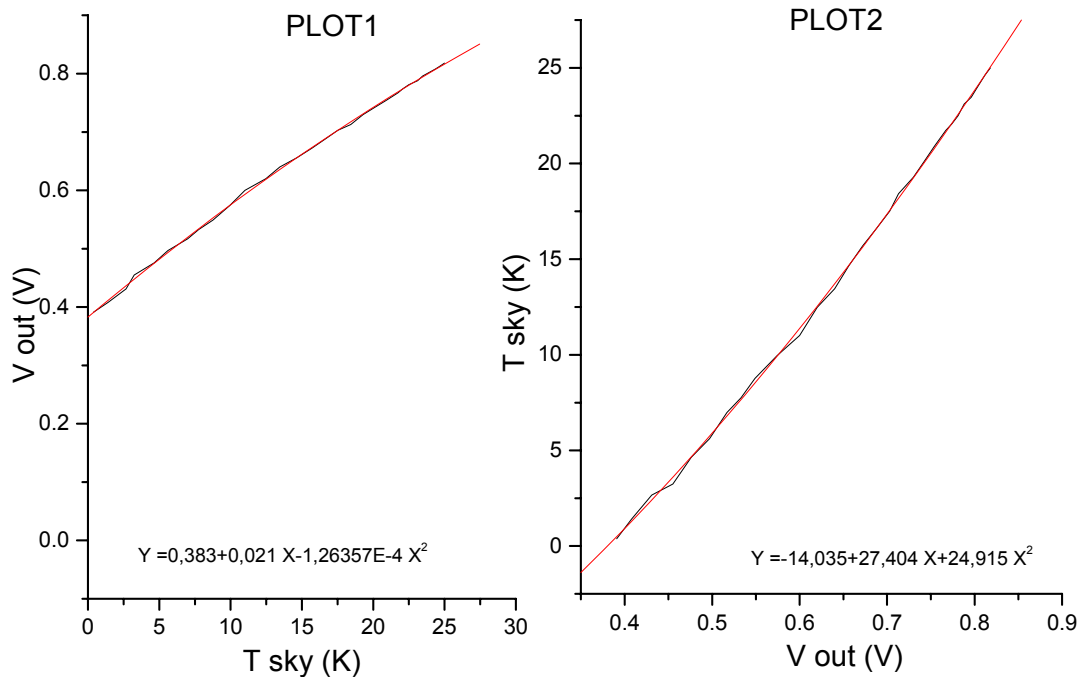


Figure 25 BEM B3 output voltages as a function of Sky temperature. In the right plot the dependence is inverted.

Experimental curves have been very well fit in both the cases using parabolic curves.

OK-25K	BEHAVIOUR	EQUATION	A	Er (A)	B1	Er (B1)	B2	Er (B2)	R-SQ
PLOT1	PARABOLIC	$Y = A + B1 * X + B2 * X^2$	0,383	0,002	0,021	3,0E-4	-1,2E-4	1,1-5	0.99999
PLOT2	PARABOLIC	$Y = A + B1 * X + B2 * X^2$	-14,035	0,730	27,404	2,439	24,915	1,961	0.99999

Table 8



The Noise Temperature has been obtained as intercept of the curves respectively with the X axis (for $Y=0$) and with the Y axis ($X=0$) .

Values found are:

$$\begin{aligned} T_n (\text{PLOT1}) &= 16.58 \text{ K} \\ T_n (\text{PLOT2}) &= 14.04 \text{ K} \\ \langle T_n \rangle_{1,2} &= 15.31 \text{ K} \end{aligned}$$

It must be noted here that, for homogeneity with JBO results, Noise Temperature is given in this document always as Thermodynamic Temperature and not as Antenna Temperature.

Gain is evaluated as the 1st derivative of the two plots; in the case of PLOT1 it is found $1/G$, then the result must be inverted. Also in this case, as made for the Noise Temperature, also the average between the two curves is evaluated. Results from this analysis are displayed in Figure 26. Differences between the two plots are instead highlighted in Figure 23.

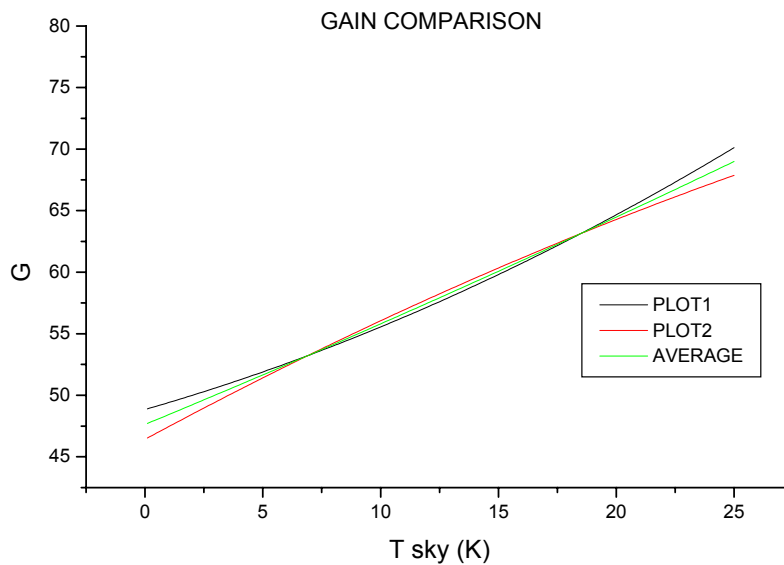


Figure 26

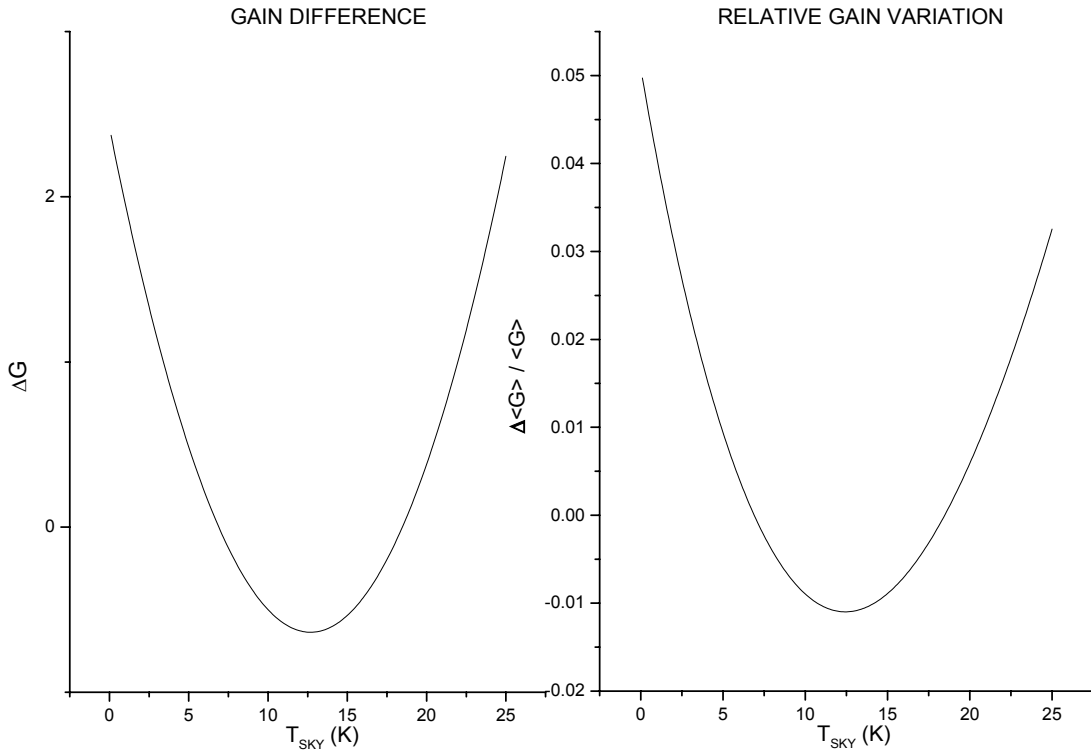


Figure 27

The Gain plots can be both fit using parabolic regressions; coefficients are given below.

$$\begin{aligned}
 G1 &= 48,842 + 0,551 * T + 0,012 * T^2 \\
 G2 &= 46,422 + 1,033 * T - 0,007 * T^2 \\
 \langle G \rangle &= 47,632 + 0,792 * T + 0,0025 * T^2
 \end{aligned}$$

The previous results are obtained considering the region [0K – 25K]; since RCA tests are allowed to explore only the range [8.5K – 25K], the above analysis is performed again limiting the fit to this range. However, it must be outlined that from 3K to 8.5 K the relative change, assuming a FEM $T_n=15K$, is only by 0.78, that is -1dB in the input power.

8K-25K	BEHAVIOUR	EQUATION	A	Er (A)	B1	Er (B1)	B2	Er (B2)	R-SQ
PLOT1	PARABOLIC	$Y = A + B1 * X + B2 * X^2$	0,389	0,007	0,019	8,0E-4	-1,0E-4	2,5E-5	0.99915
PLOT2	PARABOLIC	$Y = A + B1 * X + B2 * X^2$	-13.873	2,527	26,876	7,348	25,327	5,281	0.99928

Table 9

Values found are:

T_n (PLOT1)	18.15 K
T_n (PLOT2)	13.87 K
$\langle T_n \rangle_{1,2}$	16.06 K

Table 10



Average result changes by about 0.7 K if the range [0K – 8K] is neglected in the fit. Given the experimental accuracy, result seems to depend only weakly on it.

Only for completeness, results from this analysis are compared with preliminary results from RCA_24 calibration tests, despite the following remarkable differences in the experimental setup:

- FEM mounted on RCA-24 is 4F2, having gain about 1 dB lower than 4F3.
- BEM mounted on RCA-24 is B1, while B3 and B4 BEMs are only representative of flight BEMs. Indeed, all the flight BEMs have common general properties but slightly different characteristics.

In reason of what above, it is expected that B3 analysis be representative of general behaviour of RCA FM radiometers but with specific differences. Curves will be presented in the next paragraph compared with 4F2+B3 analysis.

11.2 4F2+ B3 analysis: JBO Test vs. RCA_24 FM

To try to recover the same instrumental setup of FM RCA_24 tests, it is here processed also a subset from data taken during the December test campaign on FEM 4F2 + BEM B3 (Channel A): the set is the same used to build the cyan curve shown in Figure 8 and in Figure 17. Voltages are plotted versus temperature using the same procedure followed in this paragraph for 4F3+B3. Output is expressed as voltage in ‘unbalanced’ conditions ($V^+ - V^0$): to be compared with 4F3 (balanced), voltage must be multiplied times 2.

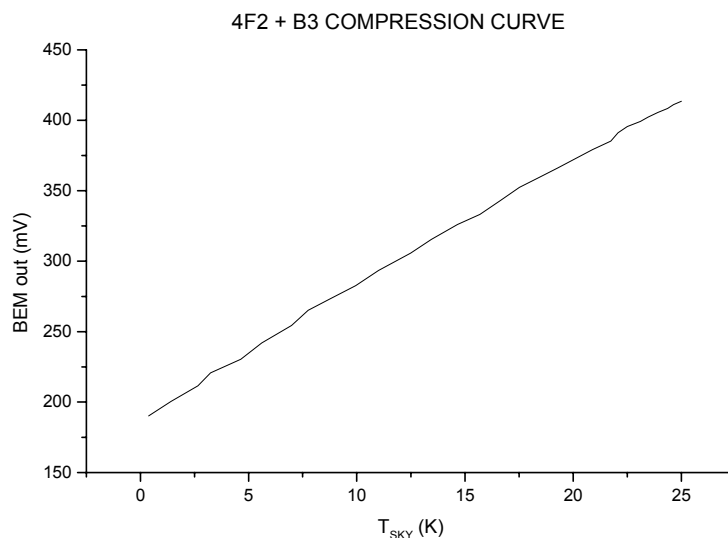


Figure 28

4F2_V_{OUT} can be renormalized to the RCA_V_{OUT} multiplying times the scaling factor S_2 :



$$S_2 = [RCA_V_{OUT} / 4F2_V_{OUT}]_{25K}$$

The same is done for 4F3 using the scaling factor S_3 :

$$S_3 = [RCA_V_{OUT} / 4F3_V_{OUT}]_{25K}$$

Results from this comparison are presented in Figure 29 ; here, measured data and parabolic fits for B3+4F2 and B3+ 4F3 are compared with RCA_24 FM results. The channel chosen is A.

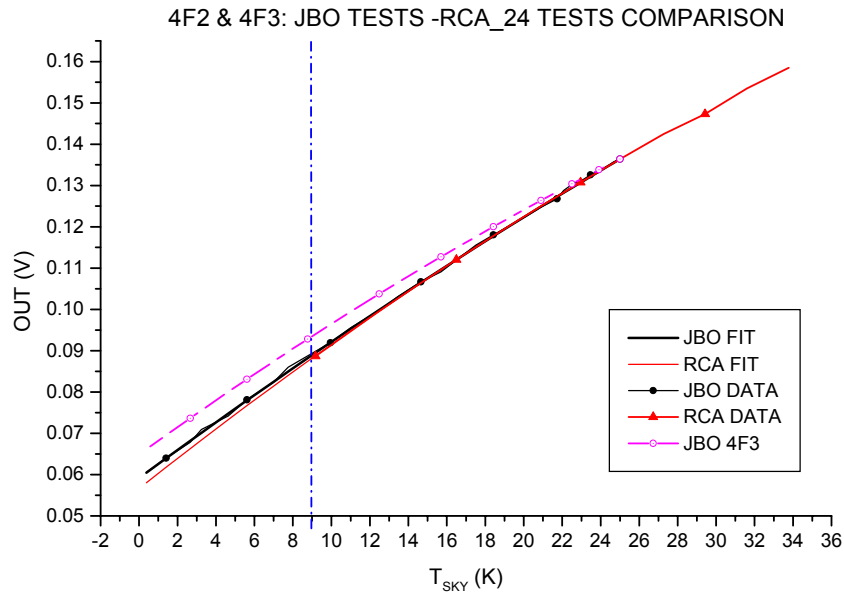


Figure 29

Plot shows that JBO measurements and RCA tests are in very good agreement within the operative range of RCA tests. However, also from 8.5K to 3K , differences are smaller than 3%, as it is shown by Figure 30.

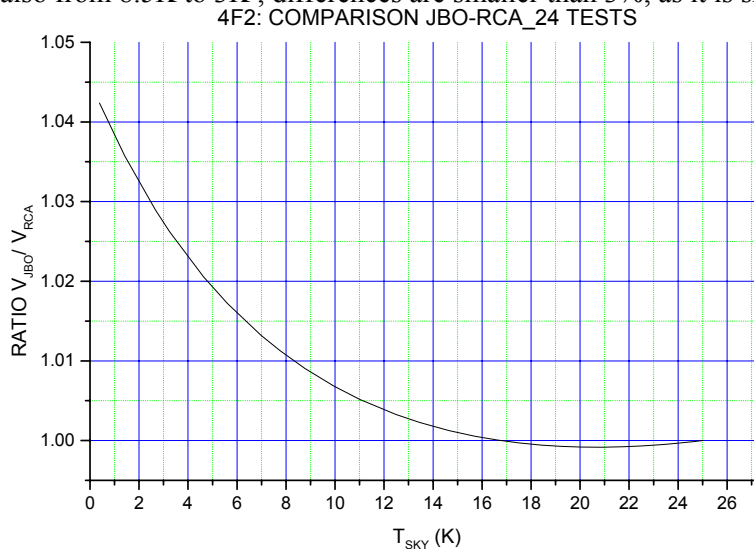


Figure 30 comparison between RCA and JBO voltages: the ratio V_{JBO}/V_{RCA} is displayed vs. T .



Following the same approach of 4F3+B3 analysis, also the curve T vs. V is plotted for JBO and RCA data. The parabolic fits used are reported in Table 11 together with Noise temperature found from curves and with their average value.

	JBO	TN	RCA	TN
V-T	$Y = 0.0566 + 0.00369X - 1.99E^{-5}X^2$	16.14 K	$Y = 0.05916 + 0.00344X - 1.383E^{-5}X^2$	14.25 K
T-V	$Y = -15.23 + 230.05X + 475.18X^2$	15.23 K	$Y = -12.77 + 191.61X + 623.68X^2$	12.77 K
<Tn>		15.6 K		13.5 K

Table 11

11.3 EXTRAPOLATION TO FLIGHT CONDITIONS

The most important question to answer is: basing on the above tests, **how compression is expected to affect radiometer performance in flight conditions?**

The scales to be investigated are mainly two:

- a region centred approximately at 3K and wide 100 mK: it represents the Sky temperature fluctuation when Jupiter enters the beam.
- A region centred approximately at 3K and wide 6 mK: it represents the temperature variation due to Dipole, when is used as calibrating source.

We want here to investigate which is the effect of considering the radiometer response linear instead of parabolic; especially we want to understand how vary the GAIN with T and what is the relative error committed on temperature effectively read from the radiometer in the two intervals considered.

In the next issue of this document it will be analysed also the impact of compression due to the radiometer being a differential receiver: also if at a first look it seems that compression does not play a role in doing the difference between T_{SKY} and T_{REF} , this feature should be carefully considered.

11.4 $T_{SKY} = 3K \pm 100 \text{ mK}$.

Compression curves are used here to investigate effects from compression in the range $T_{SKY}=[2.9K : 3.1K]$. Due to uncertainty due to experimental measurement a wider region [1.5K : 7 K] is chosen to perform the parabolic fit and only further the analysis is restricted to the chosen interval.

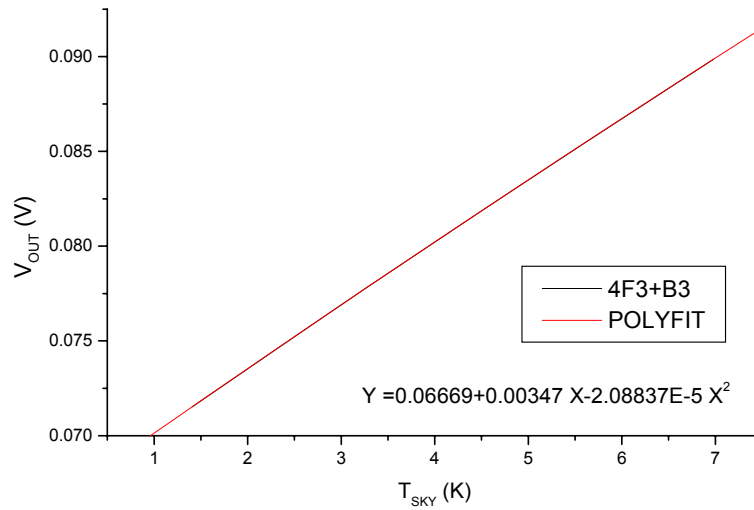


Figure 31

Experimental data have been fitted with a parabolic regression $Y = A + B1 \cdot X + B2 \cdot X^2$ having coefficients reported in table below

1.5K-7K	BEHAVIOUR	EQUATION	A	Er (A)	B1	Er (B1)	B2	Er (B2)	R-SQ
PLOT1	PARABOLIC	$Y = A + B1 \cdot X + B2 \cdot X^2$	0.06666	7.E-6	0.00347	4.E-7	-2.088E-5	3E-6	1

Table 12

The Range have been restricted to [2.9K : 3.1K] : from the derivative analysis Gain variation with T has been evaluated; results are reported in Table 13. $\delta G/G$ and $\delta T/T$ are reported both for B3 and B4; the effect of different FEM noise temperatures have been also taken into account to evaluate impact on non-linearity.

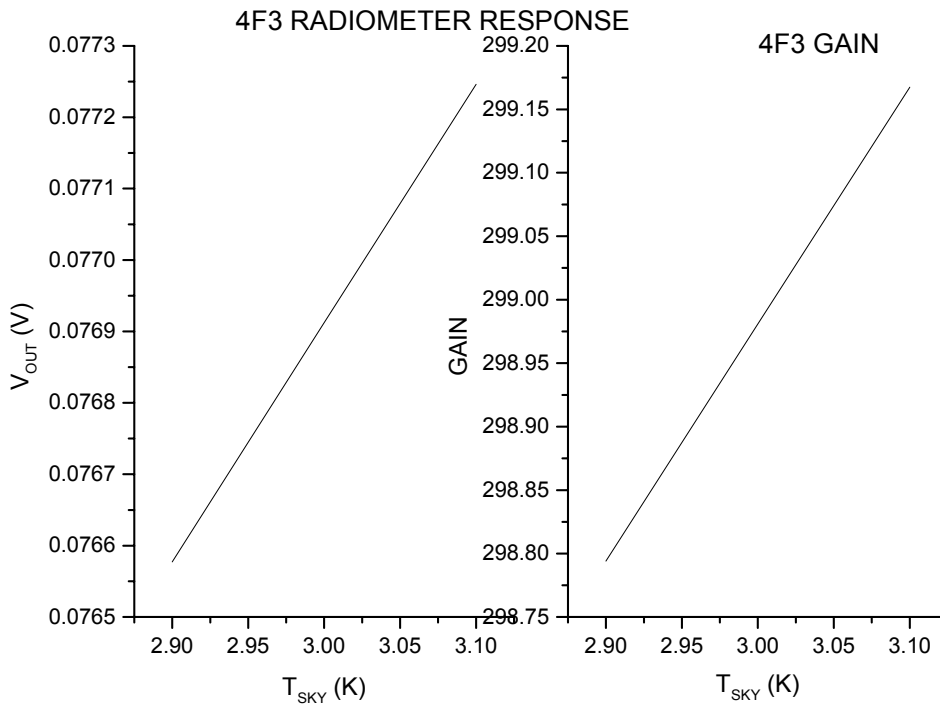


Figure 32

TNOISE (K)	DG/G	DG/G	DT'/DT	DT'/DT	DT ABS (K)	DT ABS (K)
	B3	B4	B3	B4	B3	B4
15	0.000816707	0.000773	0.999183	0.999227	8.17374E-05	7.73537E-05
18	0.000858789	0.000811	0.999141	0.999189	8.59528E-05	8.11186E-05
30	0.001081748	0.001006	0.998918	0.998994	0.000108292	0.000100729

Table 13 absolute quantities refer to a SKY temperature fluctuation of 100 mK.

11.5 $T_{SKY} = 3K \pm 3 mK$.

The same analysis of above is repeated supposing T_{SKY} having a peak to peak equal to 6 mK. Results are slightly improved with respect to the previous case.

TNOISE (K)	DG/G	DG/G	DT'/DT	DT'/DT	DT ABS (K)	DT ABS (K)
	B3	B4	B3	B4	B3	B4
15	2.45012E-05	2.32E-05	0.999975	0.999977	7.35054E-08	6.95662E-08
18	2.33779E-05	2.21E-05	0.999977	0.999978	7.01354E-08	6.62854E-08
30	1.97552E-05	1.86E-05	0.99998	0.999981	5.92666E-08	5.57658E-08

Table 14 absolute quantities refer to a SKY temperature fluctuation of 6 mK



12 SUMMARY

Here follow, briefly summarised, the main results of this work. Prototype BEMs B3 and B4 have been studied coupled to FEM 4F3 and FEM 4F2, in order to investigate the non linear relation between signal recorded (voltage) and

Power feeding the BEM from the FEM, through a variable attenuator, has been characterised using different methods: power meter, noise figure meter and VNA analysis are, in the worst case, in agreement within 3% accuracy.

Signals exiting both BEM B3 and B4 have a non linear dependence on power input (Temperature). It means that the detector is not working in square law conditions. Despite B3 and B4 have different outputs, renormalized curves have very similar shape: in both the cases the best fit is a parabolic regression $Y=A+B1*X+B2*X^2$ with coefficient $B2<0$. There is no way to fit Voltage-Power curves using a linear fit: derivative analysis has been used as powerful method to investigate also local linearity. From this analysis, it comes out that BEMs do not work in square law regime nor in linear regime but in a mixed parabolic one: it is true also within small regions of the compression curve.

1-dB compression point can not be defined unambiguously: compression curves indicate that it is impossible, using the data set employed within the interval analysed, to find uncompressed regions. This lack avoids to define the point P0-in from which to start to evaluate 1-dB compression. Anyway, B3 and B4 show to be affected by the same degree of compression.

1-dB compression research seems to be more a formal than a useful exercise, because in this case it does not add any information to characterise or solve compression problem.

Noise Temperatures, evaluated in non linear conditions using the Y-factor method, are very far from reasonable values. This is true also if the signal is reduced by interposing a variable attenuator between FEM and BEM. Indeed, it is expected to happen, since the noise component from the BEM gains as much importance as the power from the FEM is lowered. Noise Temperatures have been corrected analytically, using compression curves previously characterised, linearizing 'Hot state' voltage. This correction enables to use Y factor method as in linear conditions. Compressed noise temperatures and corrected values are reported together in the table below.

CHANNEL	COMPRESSED	CORRECTED
A	62.0 K	17.1 K
B	56.9 K	16.2 K
C	73.0 K	18.7 K
D	66.0 K	18.5 K

To check if compression could be due to a bad filtering, in the first LNA (IC1) or in the pass band filter mounted inside the BEM, a waveguide filter has been used to investigate the origin of power entering the BEM. It was found that the IC1 and pass band filter insertion gain profile are able to cut off power incoming from outside the nominal bandwidth; it has been estimated that the power excess coming from the region $Freq>48.4$ GHz can be, also in the worst case, smaller than 1.15 dB for B3 and 0.7 dB for B4.

Any attempt to build a broad band noise source representative of the FEM, using the prototype BEM44_B1_RF failed. Compression curves obtained, although the integrated power input was the same, are very different. However, this result is useful because it indicates that the BEM characterization at a single frequency using a CW single tone approach is very far to be representative of the system behaviour. This result was already evident also from the simple FEM+BEM analysis: comparison between voltages obtained



in correspondence of a broad band input power (FEM or BEM44_B1_RF) and of a CW tone at 44 GHz are very different. CW single tone approach could be much more useful if applied in sequence to many points within the nominal bandwidth: it could provide a parametric investigation of compression with frequency and input power level.

Compression curves from prototypes analysis have been managed in order to extrapolate results to : RCA_24 FM calibration tests, flight operations.

Power input has been converted into equivalent temperature from the load in the wise to draw V-T and T-V curves. Results have been renormalized to RCA_24 output and compared with. This analysis has been performed both for 4F3 FEM and for 4F2 FEM, that is the FEM mounted on the RCA_24. Comparison with a preliminary RCA analysis shows that curves are in very good agreement: it means that JBO tests on prototypes are representative of tests on the full integrated RCA. Noise temperatures have been evaluated correcting for compression with the parabolic regression within the interval [0K:25K]: values found are respectively 15.3 K (4F3) and 15.6K (4F2) in thermodynamic temperature. The same quantity, evaluated from RCA_24 data set provides $T_n=13.5$ K .

Since RCA tests, because of thermal setup limits, are performed in the range $T_{SKY}=[8.5K : 33 K]$, a sensitivity test has been done in order to evaluate T_n , if the range [0K : 8.5K] is neglected: result changes by only 0.7K. It means that also with the above experimental limits, RCA analysis is representative, with a limited uncertainty, of the behaviour expected in nominal operating conditions ($T_{SKY} = 4K$). Actually, if some error is committed due to higher T_{SKY} , it can not be able to explain a drastic change in detector behaviour.

The same analysis has been applied to flight conditions, taking into account the thermal ranges representative of main in-flight calibration operations: $T_{SKY} = 3K \pm 100$ mK (Jupiter enters the beam) and $T_{SKY} = 3K \pm 3$ mK (observing Dipole).

The relative Gain variation due to non linearity is comprised between $8E-4$ and $1E-3$ (B3) and $7E-4$ and $1E-3$ (B4): the values given depend on the FEM stand-alone noise temperature supposed, ranging in this parametric calculation from 15K to 30K. The absolute error committed in the temperature estimation of the fluctuation 100mK is always smaller than $90\mu K$.

In the case of Dipole, $\delta G/G$ ranges from $2.5 E-5$ to $1.8 E-5$ while the absolute error on temperature estimation for a fluctuation of 6mK p-p is always smaller than $0.07 \mu K$

From LFI requirements it must be always $\delta G/G < 1E-2$

13 CONCLUSIONS

Results from this work enforces to retain that the JBO analysis on prototype BEMs coupled with FM FEMs is largely representative of the non linearity in FM calibration measurements at 44 GHz. In force of what found, non linearity seems not able to cause critical problems during in-flight operations.

RCA calibration measurements are strongly dependent on non linearity, if performed on wide temperature range: final values depend on the fit employed and on the analytic approach, strongly affecting results. Anyway, if compression is considered, it is possible to estimate with a good degree of accuracy the general properties of the radiometer and to understand if it is working properly.

All above seem to indicate that a more accurate investigation of properties must be demanded to in-flight operations.